Journal of Template

Vol. 00, No. 0, 0000

Laminar-Turbulent Transition of an Inlet Boundary Layer in a Circular Pipe Induced by Periodic Ejection (Condition for Generating an Isolated Turbulent Patch)*

Masashi ICHIMIYA** Hayato FUJIMURA*** and Junji TAMATANI****

**Institute of Technology and Science, The University of Tokushima,
2-1 Minami-Josanjima-cho, Tokushima-shi, Tokushima, 770-8506 Japan
E-mail: ichmiya@me.tokushima-u.ac.jp
***Graduate School, The University of Tokushima
****Institute of Technology and Science, The University of Tokushima

Abstract

The laminar-turbulent transition of a boundary layer induced by jet flow ejection in the inlet region of a circular pipe was experimentally investigated. The jet flow was periodically inserted radially from a small hole in the inlet region into the pipe flow. Axial velocity was monitored by a hot-wire anemometer. The difference of properties in laminar-turbulent transition from developed Hagen-Poiseuille flow was examined. Isolated turbulence patches were generated by the jets, and then they propagated downstream. The leading edge of the turbulent patch was definite, whereas its trailing edge was not. This characteristic was similar to that of a turbulent spot in a flat-plate boundary layer. The threshold value of the jet flow rate to generate the turbulent patch was then obtained. The threshold value decreased and saturated finally with the increase in jet flow duration. The normalized jet flow duration when the threshold value was saturated increased with the increase in Reynolds number, contrary to the developed region. The normalized threshold flow rate tended to vary with the Reynolds number among three regions. All tendencies were different from those of the developed region. With the increase in jet flow rate beyond the threshold value, the duration of the turbulent patch increased, though the fluctuating velocity within the patch did not. The propagation velocities of the leading and trailing edges, and the duration and fluctuating velocity within the turbulent patch were almost constant irrespective of the jet flow ejection frequency.

Key words: Pipe Flow, Transition, Boundary Layer, Turbulence, Inlet Region, Isolated Turbulent Patch, Threshold Value

1. Introduction

Fully developed pipe laminar flow, i.e., Hagen-Poiseuille (hereafter HP) flow is known to be stable to axisymmetric and all type non-axisymmetric disturbance from theoretical and experimental results[(1)~(4)]. It is well known, however, that when Reynolds number exceeds its critical value, 1800-2300, an isolated turbulent patch, i.e., turbulent puff or turbulent slug appears intermittently. It gradually occupies the section perpendicular to the flow, its axial length extends, and finally the flow becomes fully turbulent downstream. This contradiction has been attributed to the fact that the finite amplitude disturbance and an inlet region

*Received XX Xxx, 200X (No. XX-XXXX)
[DOI: 00.0000/ABCDE.2006.000000]

upstream has not been considered in the theory. In the linear stability theory of HP flow the Reynolds number at which the flow becomes unstable is infinite. On the other hand, in the inlet region the critical Reynolds number is 9700[5], 19900[6] and 11700[7] based on a pipe radius and velocity which is averaged over the cross-section in the linear stability theory and approximately 7600 based on a pipe diameter in an experiment using tripping wires[8]. Therefore, roles in which the inlet region plays are critical and to clarify this role is expected. As one example of the fundamental flows such as the pipe flow, in the laminar-turbulent transition process on a flat plate boundary layer, an isolated turbulent patch, i.e., turbulent spot appears when the free stream turbulence is high[9]. The transition process proceeds as the spots grow and merge with each other. In this way, the outline of the transition process is similar in the pipe flow and flat plate boundary layer, though the wall curvature and streamwise pressure gradient are different.

Previous studies on the onset of turbulence in pipe HP flow are reviewed at first. In theoretical studies the relation between a threshold disturbance intensity needed for the onset of the turbulence, ε, and Reynolds number have been investigated[10]~[17]. In an early stage, from balances between time-derivative, nonlinear and viscous terms in Navier-Stokes equation or several estimates in a time scale in a nonlinear stability theory, ε scaled in proportion to $Re^{-1/2}$, Re^{-1}, Re^{-2} and Re^{-3}[10][18]. Then, a theory was published which suggests $\varepsilon \sim O(Re^{-3})$[11]. Recent theories showed that $\varepsilon \sim O(Re^{-1} \sim Re^{-1.5})$[12]~[17]. Next, in experimental studies as in a flat plate boundary layer, turbulent puffs or slugs have been originated artificially from forced disturbances, and then their structure and development process have been clarified[19]~[27]. Especially, jet flow disturbances which issued from a pipe wall into the main flow have been mainly used[23][28]~[32]. The threshold for the onset of turbulent patches has been scaled to $Re^{-2/3} \sim Re^{-1.5}$[28]~[32]. In their experiments, Hof et al. showed that the threshold value decreased with the jet flow duration and finally saturated, and its variation with the duration was irrespective of Re[29].

On the other hand, for the inlet region a numerical simulation about transition length[33] and recently an experiment about transition Reynolds number[34] have been published. For forced transition experiments[8][19][20][22][35]~[37], fixed bodies such as orifices have been used mainly and jets from the wall as HP flow have rarely been seen. Moreover, key observations have been conducted in the HP flow region. Additionally, threshold properties in the inlet region have not been investigated at all. In the inlet region the core contacts the boundary layer as flat plate boundary layer. Therefore, the isolated turbulent patches originated in the inlet boundary layer are expected to behave like the turbulent spots in the flat plate boundary layer rather than turbulent puffs or slugs in developed pipe flows, though the details of the turbulent patches have not been clarified. In this connection, the threshold for the origin of turbulent spots might have not have been clarified either. From this standpoint, the present authors thought that the natural transition process begins from the inlet region, then installed a single roughness element in the inlet region and studied a steady turbulent region which was formed downstream of the roughness element[38].

In the present investigation, a jet flow disturbance was introduced periodically in the inlet region, and then the threshold value of the jet flow rate to produce the isolated turbulent patches in the boundary layer was obtained as a function of a Reynolds number and jet flow duration. Observations were also conducted in the inlet region, and then the results were compared with those in the HP flow. The subject of observations in HP flow covers whole sections which are perpendicular to the main flow. On the other hand, in the present investigation isolated turbulent patches in the boundary layer were observed exclusively, though a few whole sections were also observed. In addition, the isolated turbulent patches originated by a larger jet flow rate above the threshold, and the effects of the jet flow rate and jet frequency on the properties of the turbulent patches were studied.

Nomenclature

a, D : pipe radius = 30 mm and diameter = 60 mm
C_{pw} : static pressure coefficient = $(p - p_0)/(\rho U_a^2/2)$
f_j : combination frequency of jet flow ejection and non-ejection = $1 / T_j$
I : intermittency function
p, p_0 : static pressure and its value at $x = 0$
Q_j, $Q_{j,crit.}$: jet flow rate during ejection into pipe and its threshold value for the origin of isolated turbulent patch
Q_p : pipe flow rate = $(\pi/4)D^2U_a$
Re : Reynolds number = $D\,U_a / \nu$
T_j : combination time period of jet flow ejection and non-ejection = $\tau_1 + \tau_2 = 8\tau_1$
$\tilde{u}$: axial instantaneous velocity
U, u : axial mean velocity and its deviation
u' : root mean square value of u
U_a, U_c : velocity averaged over the cross-section and centerline velocity
U_e : velocity at edge of boundary layer
x, y : coordinate system, see Fig. 1
x_j : station of jet flow ejection = 107 mm
δ : boundary layer thckness defined by $U / U_e = 0.995$
θ : peripheral angle from jet flow hole
ν : kinematic viscosity of air
ρ : density of air
τ_1, τ_2: jet flow ejection and non-ejection durations into pipe
$<*>$: ensemble average of quantity $*$

2. Experimental Apparatus and Methods

A plexiglas pipe with a diameter, D, of 60 mm and a total length of approximately 6.2 m (= 104D) was used in the experiment. A fan downstream of the pipe sucked air into the pipe. Six pipes 1 m in length are connected smoothly. The axisymmetry of the axial velocity was satisfactory.

Figure 1 shows the coordinate system and flow field. An axial coordinate, x, starts from a position where the curvature of an inlet bell-mouth curve becomes straight. The bell-mouth was made smoothly and the curve adopted was according to Ito et al.[39] so as not to make a separation. The origin of the coordinate is 90 mm downstream from the inlet. The radial coordinate, y, starts from the wall surface and the peripheral angle, θ, starts from the jet flow hole mentioned later. As a point disturbance, a single jet flow was ejected orthogonal to the main flow through a 2 mm diameter hole 107 mm downstream of the coordinate origin, as shown in Fig. 1.

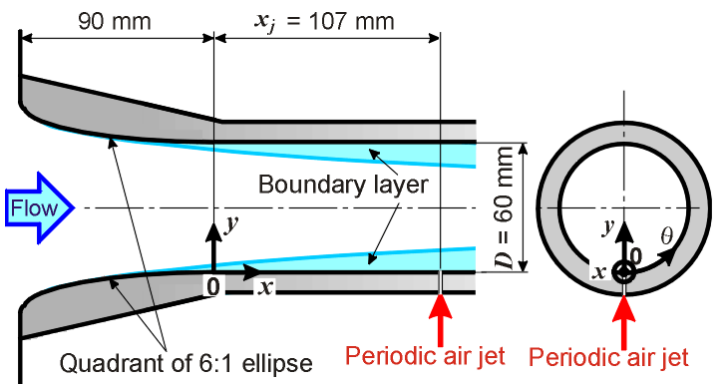

Fig. 1 Coordinate system and air jet.

Air came from an air pump (Suisaku Co., Ltd., SSPP-3) is led to a solenoid valve (SMC Co., Ltd., VT301). Two air exits from the valve are interchangeable periodically; one is connected to the jet flow hole on the pipe wall, another is exhausted outside of the pipe. The exits are changed at the moment that direct current voltage which changes from low to high supplied into the valve and at the reverse moment. To generate the direct current, a photointerrupter is used. Light beam emitted from an LED is interrupted periodically. To make the interruption, a disk with a sector-shaped notch rotates around its center at a constant speed. The center angle of the notch sector is 45° and that of the sector without the notch is 315°. The rotation of the disk causes the interruption of the light beam. The ratio without and with interruption hours equals the angle of the sector with and without the notch, 1:7. Therefore, the ratio of jet flow ejection hours, τ_1, and no ejection hours, τ_2, becomes 1:7. When the disk rotation speed is changed, the hours τ_1 and τ_2 can be changed with the ratio of them unchanged. The air flow rate from the air pump can be changed by supplying various alternating current voltage to the pump. The relationship between the input voltage and output air flow rate has been calibrated by collecting the air exhausted into water from the pump and measuring its volume.

The velocity averaged over the pipe cross-section has been decided from measurement of velocity distribution at x/D = 86. The Reynolds number, *Re*, based on the pipe diameter and the velocity averaged over the cross-section is kept 10000 ($U_a \simeq$ 2.5 m/s) excluding §3·3. In our previous experiments with a single roughness element on the pipe wall and resulting steady turbulent region, *Re* was 20000[38]. To avoid effects of natural transition on the present experiment, *Re* is lowered.

A single hot-wire probe with a tungsten sensing element 5 μm in diameter and 1 mm in length was used in the measurements. Axial velocity measurements were made with the probe on the jet flow hole generator, i.e., $\theta = 0°$. The output voltage from the hot wire had been digitized at a 10 kHz sampling frequency and a 52-second sampling period. A conventional time averaging and an ensemble averaging based on the output voltage from the photointerrupter were both performed. The sampling period corresponds to 65 times of the ensemble average. This number is estimated as sufficient from preliminary tests. Moreover, the number is approximately the same as that in the previous experiment[37].

To distinguish the flow as laminar or turbulent, various methods have been proposed so far[40)~(42)]. In the present experiment, as a simple way, a one-order time derivative of axial fluctuating velocity is compared with a constant threshold value which has been judged as valid from many comparisons between the discrimination results and instantaneous velocity signals. In this way, if the derivative exceeds the threshold value the intermittent function, *I*, was set as unity, or otherwise set as zero at the time. The time-averaged intermittent function is intermittency factor, γ, which is often used in stationary flows, though it was not obtained in the present experiment.

3. Results and Discussion

3.1 Outline of Pipe Flows Without Jet Injection

First, experimental results of the present pipe flows without jet flow ejection are briefly discussed. The Reynolds number is 10000. In the previous paper, properties of natural transition with *Re* = 20000 have been described[38].

Time-averaged mean and fluctuating velocity distributions at 7 stations are shown in Figs. 2 and 3. The theoretical velocity distribution by Tatsumi[43] in the inlet region is also shown in Fig. 2. Experimental mean velocities almost coincide with the theoretical profile during the whole pipe length. Also, during the whole length, the fluctuating velocity is rather low, thereby maintaining laminar flow at *Re* = 10000. The experimental result with

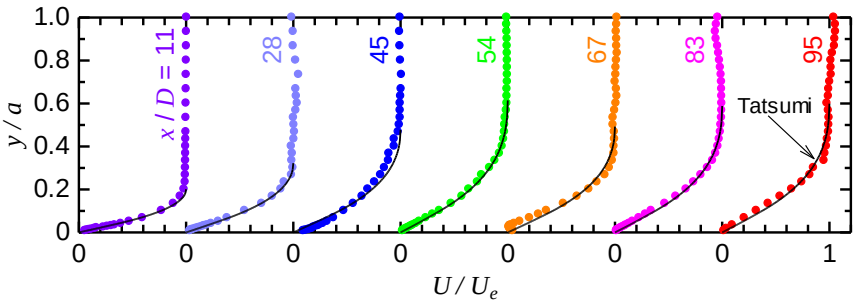

Fig. 2 Mean velocity profiles.

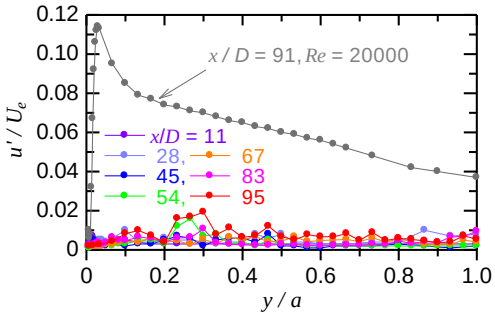

Fig. 3 Distribution of u'-fluctuating velocity component.

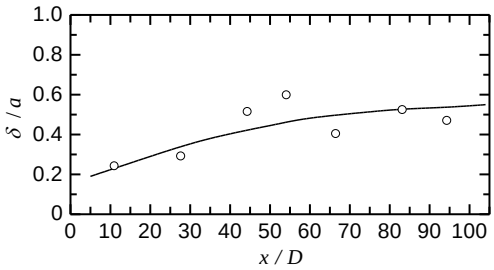

Fig. 4 Distribution of boundary layer thickness.

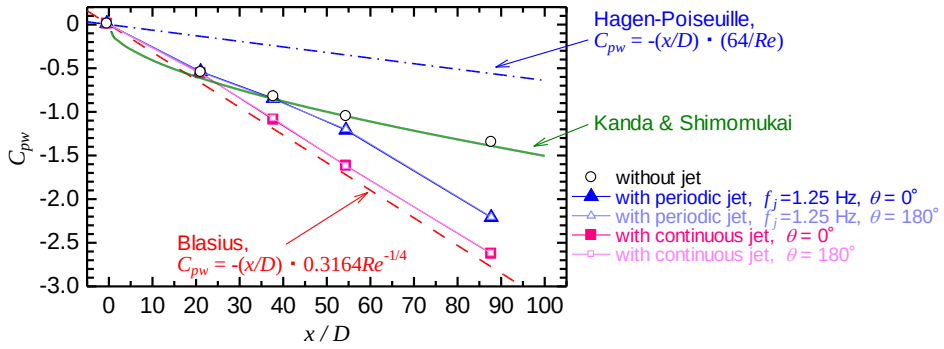

Fig. 5 Distribution of wall pressure.

Re = 20000 at x/D = 91[38], also shown in Fig. 3, indicates that in this case the turbulent transition occurs on the way there.

Figure 4 shows downstream development of the boundary layer thickness. The solid line shows the smoothed experimental results. Even near the end of the pipe (x/D = 104), the boundary layer does not reach the pipe centerline, y/a = 1, showing that the inlet region persists along the whole length. When the jet flow is ejected from the pipe wall, as shown in the next section an isolated turbulent patch develops in the boundary layer within which the boundary layer thickens. Far downstream, the turbulent patch extends axially and amalgamates with adjacent patches, thus forming developed flow before the end of the pipe. Note that all experimental results from the next sections are obtained in the relatively upstream inlet region.

Figure 5 shows axial distribution of wall pressure. As for the wall pressure shown by x in Fig. 5, we first obtain the difference in wall pressure where x = 0. Then, we normalize the distribution with the dynamic pressure based on the velocity averaged over the cross-section. The present results well coincide with the numerical result of Kanda and Shimomukai at Re = 10000 in the inlet region[44], where a velocity gradient is limited within the boundary layer, thus making it steeper than the HP flow. Therefore, the pressure loss becomes greater than that in HP flow. The loss is expressed as the $U_a^2/2$ times constant[45].

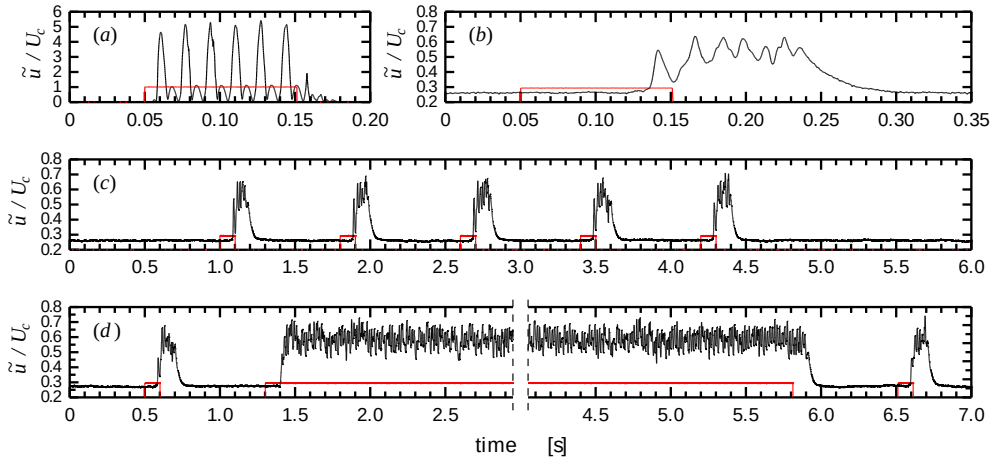

Fig. 6 Instantaneous velocity signals of small jet flow measured on the centerline of the jet flow hole and isolated turbulent patches measured at $(x-x_j) / D = 2.5$, $y/a = 0.03$, $\theta = 0°$.

The present pressure approaches the HP value minus $U_a^2/2$ times constant, though the constant is smaller than the described value[45]. Values with jet flow ejection with the flow rate, $Q_j/Q_p = 8.0 \times 10^{-4}$, which is above the threshold in this Re, are also shown in Fig. 5. Due to the periodic turbulent patches with ejection, the pressure loss increases. With continuous jet flow ejection, continuous turbulence results as shown later in Fig. 6(d), and the loss increases and approaches Blasius formula.

3.2 Outline of Isolated Turbulent Patch within Boundary Layer Produced by Jet Injection

In this section, properties of isolated turbulent patches originating within the boundary layer due to the jet flow ejection are examined. Figure 6 shows instantaneous velocity signals which contain the turbulent patches. Red rectangles indicating the lower side in each figure indicate the duration when the jet flow is ejected from the solenoid valve to the pipe, τ_1, 0.1 second.

To estimate the jet flow velocity exhausted from the air pump, the jet flow was directed to another hole with the same diameter as the pipe wall hole, and then its centerline velocity was measured 1 mm away from the hole by a hot-wire anemometer. The velocity is shown in Fig. 6(a). For 0.1 second, the air is not jetted continuously; high speed air about five times and low speed air about one times the pipe centerline velocity, U_c, are respectively ejected at the rate of 60 Hz (0.017 second each), alternatively. The mean velocity during 0.1 second becomes about 1.8 times as large as U_c. It also becomes about 2.3 times as large as the mean velocity over the cross-section of the jet flow hole. The reason for such a large value was because it was measured on the centerline of the hole. In the power spectrum of the fluctuating velocity, peaks are observed at frequencies of 60 Hz and its multiples, since in the structure of the air pump a diaphragm acts by alternating current. To check whether the air ejected with 60 Hz can be unstable and produce the turbulent patch finally, an axial wavenumber was calculated from the frequency of 60 Hz and the velocity averaged over the cross-section of the pipe, U_a. The wavenumber and displacement thickness Reynolds number at the jet flow ejection station, x_j = 107 mm fell within the stable domain of Tatsumi's stability diagram[5]. Therefore, the development and interior characteristics of the isolated turbulent patch may not be affected by the periodic fluctuation of 60 Hz but rather by the flow rate above the threshold. The time when the air starts ejection, 0.06 second, is 0.01 second later than when the solenoid valve directs air in the pipe direction, for 0.05 second, due to the tube length 400 mm between the solenoid valve and the jet flow hole on the pipe wall.

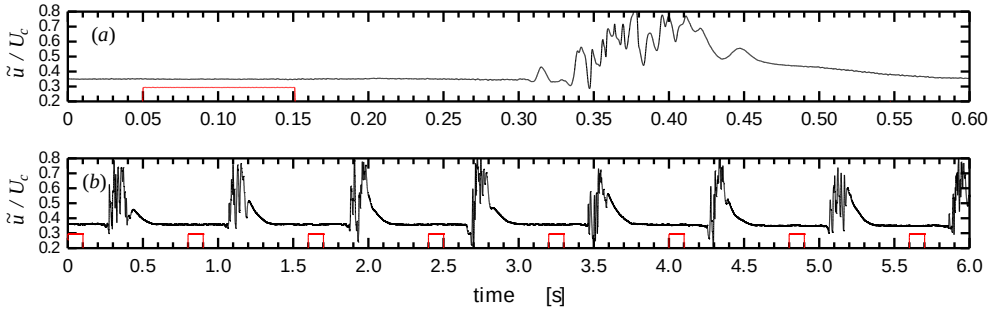

Fig. 7 Instantaneous velocity signals of small jet flow and isolated turbulent patches measured at $(x-x_j)/D = 9.4$, $y/a = 0.04$, $\theta = 0°$.

In Fig. 6(*b*), (*c*) and (*d*), instantaneous velocity signals including the isolated turbulent patches are shown which are observed at the height of maximum fluctuating velocity, y/a = 0.03, at $(x - x_j)/D = 2.5$, $\theta = 0°$. The jet flow is ejected at the rate of $f_j = 1.25$ Hz($\tau_1 = 0.1$ second) and the Reynolds number, 10000. The jet flow rate Q_j/Q_p is 8.2×10^{-4}, which is higher than the threshold shown later. In Fig. 6(*b*), a single isolated turbulent patch can be seen. The time when the leading edge, i.e., downstream edge of the patch appears, is 0.05 second later than the time when the solenoid valve introduces air into the jet flow hole, since it needs to travel the tube length in Fig. 6(*a*) plus axial distance 2.5*D* after it is ejected into the pipe. The periodicity of 60 Hz shown in Fig. 6(*a*) still can be seen here even after the patch traveled for the axial distance of 2.5*D*. Among the turbulent patches in the developed region, turbulent puffs have an indefinite leading edge and a definite trailing (upstream) edge; on the other hand, in turbulent slugs both edges are definite[19][23][37]. Present turbulent patches have a definite leading edge, though in the trailing edge the velocity gradually changes. This character is similar to the turbulent spots in a flat plate boundary layer[46]. The relationship between the characteristics of these leading/trailing edges among the turbulent puffs, slugs and spots has not been explained definitely. Recently, the role of vortex shedding from wall-attached shear layers to the formation of the puffs and slugs has been suggested[47]. How the approach can be extended to the present turbulent patches is interesting. Figure 6(*c*) contains turbulent patches with five ejections. Five turbulent patches corresponding to the ejection originated. The longer ejection time of approximately 4.5 seconds in Fig. 6(*d*) produces a longer turbulent patch.

Figure 7 shows a downstream turbulent patch at $(x - x_j)/D = 9.4$, $\theta = 0°$, $y/a = 0.04$, Re = 10000, $Q_j/Q_p = 7.9\times10^{-4}$. In Fig. 7(*a*), a single isolated turbulent patch is shown. More time for arrival there requires a greater axial distance. The periodicity of 60 Hz cannot be seen here. Actually, among the power spectrum peaks, those at $(x - x_j)/D = 2.5$ were no longer seen. Figure 7(*b*) shows multiple patches with periodical jet flow ejection. The duration of the patch is longer than that in Fig. 6 because of the difference in velocity between the leading and trailing edges as well as turbulent slugs. The velocity of both edge and expansion of the patches will be reported in the future. Though velocity fluctuations can still be seen at the centerline of the pipe, from the intermittency factor (not shown here), the turbulent patch did not reach the centerline on the meridian plane including the centerline. Hence, the turbulent patches remain within the boundary layer relatively upstream. The shape of the patches will also be shown in the future.

3.3 Threshold Flow Rate for Origin of Turbulent Patch in Boundary Layer

The threshold jet flow rate, $Q_{j,crit.}$, i.e., lower limit for the onset of the isolated turbulent patches, will be examined here. First of all, fluctuating velocity from an ensemble-averaged velocity, $\hat{u}$ is obtained at every instance. Then, the fluctuating velocity is squared and ensemble-averaged, i.e., $<\hat{u}^2>$. If its square root more than doubles in a laminar time domain in this position, the turbulent patch is regarded as having been produced. In many

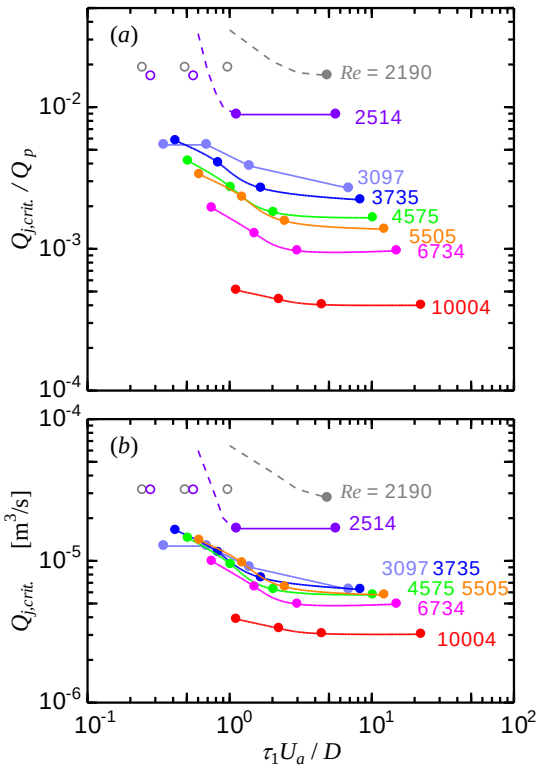

Fig. 8 Threshold jet flow rate against normalized jet flow duration measured at $(x-x_j) / D = 15$, $y/a = 0.03$, $\theta = 0°$.

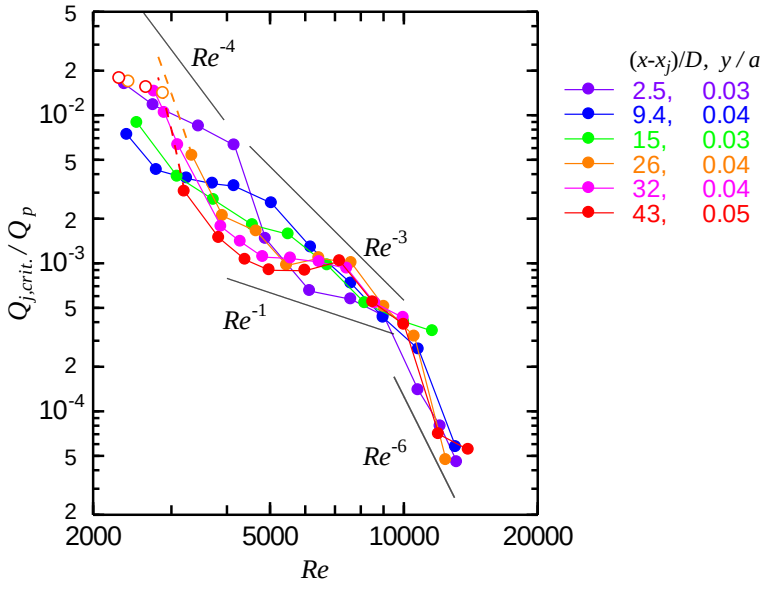

Fig. 9 Normalized threshold jet flow rate as a function of Reynolds number.

previous experiments about threshold value, the origin of turbulence was judged visually. In the present study, the fluctuating velocity is adopted since the turbulence within the patch is important. The value, 2, was decided from many comparisons between non-production and production. The comparison was easier especially in a high *Re* case and downstream, e.g., Fig. 11(*c*) and (*d*). Figure 8 shows the threshold flow rate as a function of normalized jet flow duration measured at $(x - x_j)/D = 15$, $y/a = 0.03$, $\theta = 0°$. Five cases in which turbulent patches did not originate even with maximum flow rate of the air pump are indicated as open symbols. The threshold normalized by the pipe flow rate in Fig. 8(*a*) decreases with

Re. The variation with *Re* is examined in detail in Fig. 9. The threshold without normalizing in Fig. 8(*b*) also decreases with *Re*. Also, the threshold decreases with the jet flow duration and saturates where the duration is large. The duration at which the threshold saturates increases with *Re*. In HP flow, the threshold also saturated at a large duration, though the normalized duration at which the threshold saturated was constant, approximately 6, regardless of *Re*[29]. In Ref. (29) the relationship between non-normalized threshold and normalized duration was one. The present results in the inlet region are different from those in HP flow.

Variation of the normalized threshold with *Re* is shown in Fig. 9. To determine the threshold definitely, it was measured at a height at which the fluctuating velocity becomes maximum at $\theta = 0°$ in each $(x - x_j)/D$. The jet flow duration τ_1 is 0.1 second. Division into three *Re* regions helps to examine results. First, for *Re* smaller than 4000, the threshold scales in proportion to Re^{-3}~ Re^{-4}. Since the threshold becomes infinite near the critical Reynolds number (1800~2300), the gradient thus becomes large. Actually, broken imaginary lines become steeper with the aid of four open symbols in which turbulent patches did not originate even at the maximum flow rate.

Second, in a region of $4000 < Re < 10000$, the tendency is different between upstream and downstream. For $(x - x_j)/D \leqq 15$, the threshold scales in proportion to Re^{-3} unlike HP flow; however, for $32 \leqq (x - x_j)/D$, it scales in proportion to Re^{-1}, showing that even in the inlet region the tendency becomes similar to HP flow.

Last, for $10000 < Re$, the gradient is large and the threshold scales in proportion to Re^{-6}. The boundary layer is thin due to large *Re*, so the tendency may be completely different from HP flow.

In this way, the present experimental result in the inlet region shows the threshold scales in $Re^{-\gamma}$ as well as experiments in the developed region[28]~[32] and theoretical analysis[10]~[18].

The manner of appearance of the turbulent patches is different between just behind the jet flow hole and downstream and also different between low and high *Re*. Figure 10 shows instantaneous velocity signals just behind the jet flow hole. In Fig. 10 (*a*) and (*b*), the jet flow rate is under and above the threshold, respectively, in low *Re*. Even under the threshold (*a*), velocity increase is observed periodically with the jet flow ejection. They had not been regarded as the turbulent patches because of the low fluctuating velocity within them. Above the threshold (*b*), however, fluctuating velocity within the patches are so large that they are regarded as turbulent patches, though the velocity increase is not so different from (*a*). On the other hand, in high *Re* and under the threshold (*c*), periodic variation can be seen as low *Re*. Above the threshold (*d*), however, the velocity increase becomes larger and there is larger fluctuating velocity within the patches.

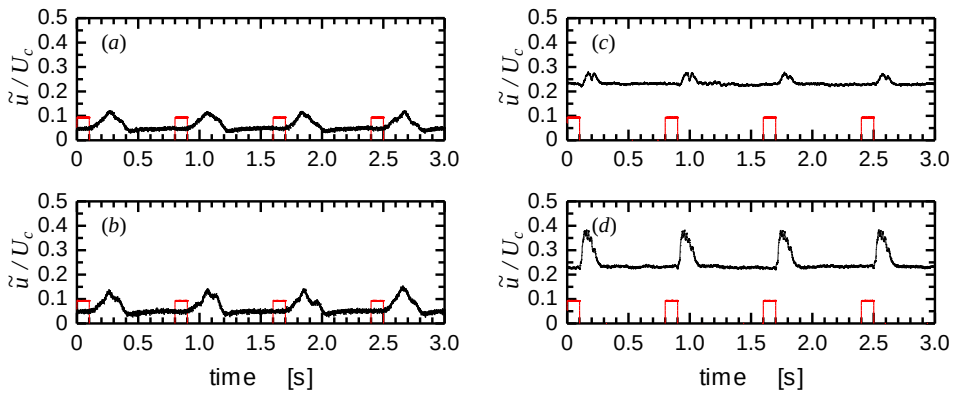

Fig. 10 Instantaneous velocity signals measured at $(x - x_j) / D = 2.5$, $y/a = 0.03$, $\theta = 0°$: (*a*) *Re* =3458, $Q_j/Q_p = 7.1\times10^{-3}$; (*b*) Re = 3458, $Q_j/Q_p = 8.7\times10^{-3}$; (*c*) *Re* = 9008, $Q_j/Q_p = 3.3\times10^{-4}$; (*d*) Re = 9008, $Q_j/Q_p = 4.6\times10^{-4}$.

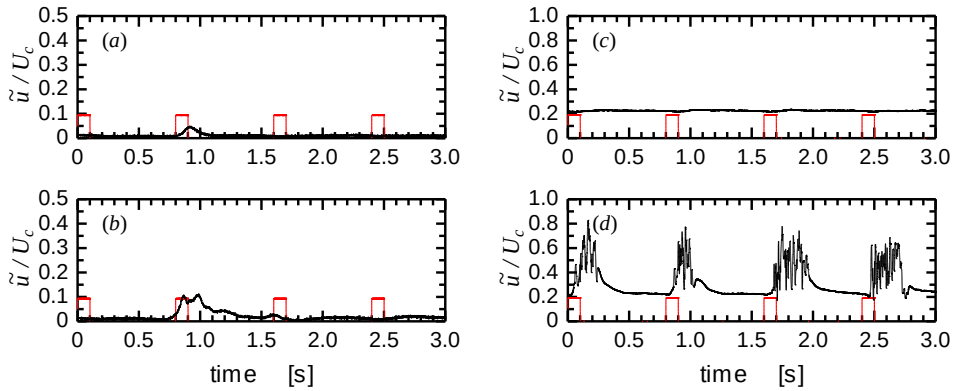

Fig. 11 Instantaneous velocity signals measured at $(x-x_j)/D = 32$, $y/a = 0.04$, $\theta = 0°$: (*a*) $Re = 2895$, $Q_j/Q_p = 1.0\times10^{-2}$; (*b*) $Re = 2895$, $Q_j/Q_p = 1.2\times10^{-2}$; (*c*) $Re = 8613$, $Q_j/Q_p = 5.3\times10^{-4}$; (*d*) $Re = 8613$, $Q_j/Q_p = 5.4\times10^{-4}$.

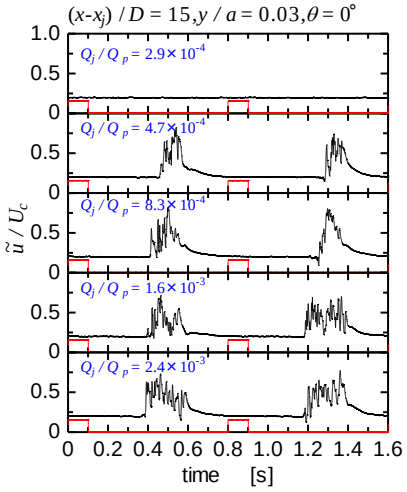

Fig. 12 Instantaneous velocity signals of isolated turbulent patches measured at $(x-x_j)/D = 15$, $y/a = 0.03$, $\theta = 0°$.

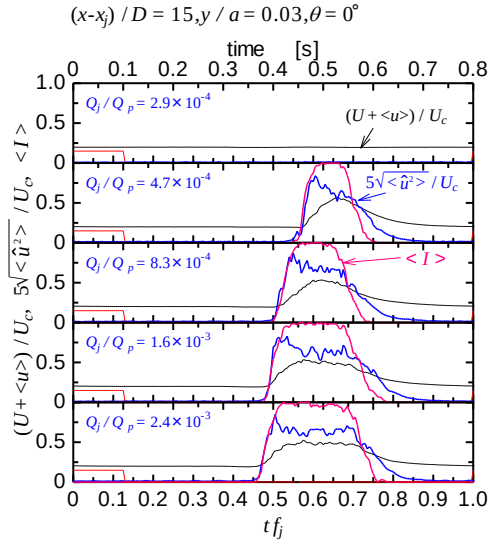

Fig. 13 Ensemble-averaged mean and fluctuating velocity components and intermittency function measured at $(x-x_j)/D = 15$, $y/a = 0.03$, $\theta = 0°$.

Figure 11 shows instantaneous velocity signals downstream. In low *Re* and under the threshold (*a*), velocity increase is sometimes observed. For above the threshold (*b*), the velocity increase becomes larger and fluctuation within the patch is larger, though the velocity increase does not necessarily always appear. In high *Re* and slightly under the threshold (*c*), no turbulent patch can be seen. For slightly above the threshold (*d*), definite turbulent patches with large fluctuation appear every time. In this way, in high *Re* if the jet flow rate exceeds the threshold slightly, definite turbulent patches appear suddenly.

3.4 Effect of Jet Flow Rate on Properties of Isolated Turbulent Patch in Boundary Layer

In this section when the isolated turbulent patch is produced with a jet flow rate above the threshold, the effects of flow rate on the fluctuating velocity within and the duration of the isolated turbulent patch are examined. Measurements were performed at the maximum fluctuating velocity, $y/a = 0.03$, at $(x - x_j)/D = 15$, $\theta = 0°$, $Re = 10000$. The jet flow duration τ_1 was 0.1 second, i.e., the combined time of the period of jet flow ejection and non-ejection into pipe was 0.8 second.

Instantaneous velocity signals for five flow rates within 2 periods, i.e., 1.6 second, are

shown in Fig. 12. The threshold, $Q_{j,crit.}/Q_p$, at this position and *Re* is approximately 4.0×10^{-4} as shown in Fig. 9. Slightly over the threshold, isolated turbulent patches appear definitely because of high *Re* as Fig. 11(*c*) and (*d*).

To examine the duration and fluctuation of the turbulent patches quantitatively, ensemble-averaged results for approximately 65 patches are shown in Fig. 13. The time is expressed for one period, i.e., 0.8 second. In Fig. 13, first an ensemble-averaged velocity is shown in black lines. Next, its deviation, i.e., fluctuating velocity is squared, then ensemble-averaged and shown in blue lines. Finally, an ensemble-averaged intermittency function is drawn in red lines. The abscissae are the real and normalized elapsed time from the jet flow ejection time, respectively. First, duration of the turbulent patches is examined for four flow rates at which the turbulent patches originate. If we regard the time range in which the ensemble-averaged intermittency function exceeds 0.5 as the duration, they were 0.098, 0.126, 0.175 and 0.188 seconds in the order of the flow rate increase, respectively. The increase of the duration with the flow rate means that as the jet flow is ejected strongly the turbulent patch lengthens at least in the axial direction. Next, for the ensemble-averaged fluctuation $<\tilde{u}^2>$, if it is averaged within the range of $<I> \geqq 0.5$, then normalized by U_c^2 and its square root is taken finally, the values were 0.131, 0.138, 0.131 and 0.129 in the increasing order of the flow rate, respectively; that is, it always remains constant. In summary, the increase in jet flow rate does not change the velocity fluctuation within the turbulent patches but lengthens their duration.

3.5 Effect of Jet Injection Frequency on Properties of Isolated Turbulent Patch in Boundary Layer

Finally, the combined frequency of the jet flow ejection and non-ejection into the pipe was varied as 0.25, 0.5, 1.25, 2.5 and 5 Hz; that is, the jet flow duration τ_1 were 0.5, 0.25, 0.1, 0.05, 0.025 seconds. Measurements were performed at $y/a = 0.05$, at $(x - x_j)/D = 15$, $\theta = 0°$, $Re = 10000$. The jet flow rate, Q_j/Q_p, was 8.2×10^{-4} and well above the threshold.

Figure 14 shows instantaneous velocity signals. The starting time is at the first ejection of the jet flow. For all jet flow rate the first isolated turbulent patch appears approximately 0.4 second after.

Figure 15 shows ensemble-averaged velocities. One period of non-normalized time was drawn in each flow rate. The appearance times of the leading and trailing edge, t_l, t_t, were regarded as when $<I>$ becomes 0.5 at first and last, respectively. The leading edge time, τ_l,

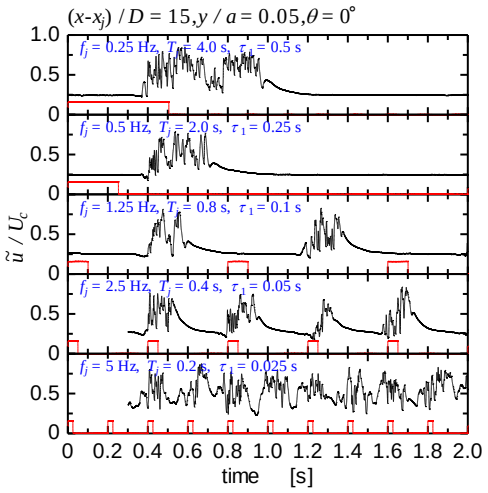

Fig. 14 Instantaneous velocity signals of isolated turbulent patches measured at $(x-x_j)/D = 15$, $y/a = 0.05$, $\theta = 0°$.

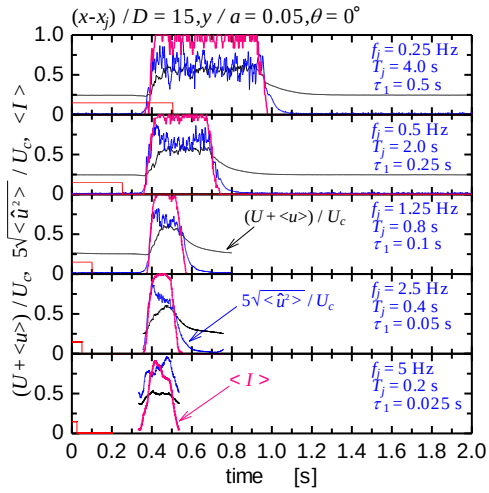

Fig. 15 Ensemble-averaged mean and fluctuating velocity components and intermittency function measured at $(x-x_j)/D = 15$, $y/a = 0.05$, $\theta = 0°$.

is constant for all frequencies and approximately 0.40 ~ 0.41 second. If we subtract t_1 and the jet flow duration τ_1, i.e., duration of red rectangle in each figure from t_t, it corresponds to the time for the growth of the turbulent patch in the axial direction while it proceeds for 15D downstream. The growth time is also almost constant for all frequencies. The previous section square root of average $<\hat{u}^2>/U_c^2$ was obtained within the range of $< I > \geqq 0.5$. They were 0.126, 0.135, 0.134, 0.140 and 0.167 in the increasing order of frequency, respectively. The larger value of the last is attributed to the fact that adjacent turbulent patches begin to amalgamate as can be seen in Fig. 14. In summary, the combination frequency of jet flow ejection does not affect the propagation velocity of the leading and trailing edges, and the duration and velocity fluctuation within the turbulent patches.

4. Conclusions

In the pipe inlet region, the jet flow was periodically and perpendicularly ejected into the main flow, then isolated turbulent patches were produced. Conditions of the jet flow rate for generating the turbulent patches were obtained in the inlet region. Also, variation in the turbulent patch with the jet flow rate and ejection frequency was examined. The following conclusions were obtained.

(1) The threshold jet flow rate for generating the isolated turbulent patches decreases with the jet flow duration and it finally saturates. The normalized time when the threshold saturates increases with the Reynolds number contrary to HP flow. The threshold decreases with the Reynolds number.

(2) The variation of normalized threshold with the Reynolds number can be classified into three regions. For $Re < 4000$, the threshold scales in proportion to $Re^{-3} \sim Re^{-4}$. For $4000 < Re < 10000$, it scales in proportion to Re^{-3} in upstream and Re^{-1} in the same way as HP flow in downstream. For $10000 < Re$, it scales in proportion to Re^{-6}.

(3) The leading edge of the turbulent patch is definite, though in the trailing edge the velocity gradually decreases. This character cannot be seen in the turbulent puffs and slugs in HP flow but is similar to the turbulent spots in the flat plate boundary layer.

(4) Once the turbulent patch appears, if the jet flow rate increasing the velocity fluctuation within the patch does not change, the duration of the turbulent patch increases.

(5) The combination frequency of jet flow ejection does not affect the propagation velocity of the leading and trailing edges, duration and velocity fluctuation within the turbulent patches.

Acknowledgments

The authors appreciate the kind instruction and constant encouragement of Prof. I. Nakamura, Nagoya University. The assistance of Messrs. H. Matsudaira and H. Ohno of the University of Tokushima is also gratefully acknowledged.

References

(1) Kerswell, R. R., Recent Progress in Understanding the Transition to Turbulence in a Pipe, *Nonlinearity*, Vol. 18, No. 6 (2005), pp. R17-R44.

(2) Eckhardt, B., Schneider, T. M., Hof, B. and Westerweel, J., Turbulence Transition in Pipe Flow, *Annual Review of Fluid Mechanics*, Vol. 39 (2007), pp. 447-468.

(3) Eckhardt, B., Turbulence Transition in Pipe Flow: Some Open Questions, *Nonlinearity*, Vol. 21, No. 1 (2008), pp. T1-T11.

(4) Willis, A.P., Peixinho, J., Kerswell, R. R. and Mullin, T., Experimental and Theoretical Progress in Pipe Flow Transition, *Philosophical Transactions of the Royal Society*, *A*, Vol.

366 (2008), pp. 2671-2684.
(5) Tatsumi, T., Stability of the Laminar Inlet-flow Prior to the Formation of Poiseuille Regime, II, *Journal of the Physical Society of Japan*, Vol. 7, No. 5 (1952), pp. 495-502.
(6) Huang, L. M. and Chen, T. S., Stability of the Developing Laminar Pipe Flow, *The Physics of Fluids*, Vol. 17, No. 1 (1974), pp. 245-247.
(7) Gupta, S. C. and Garg, V. K., Effect of Velocity Distribution on the Stability of Developing Flow in a Pipe, *The Physics of Fluids*, Vol. 24, No. 4 (1981), pp. 576-578.
(8) Sarpkaya, T., A Note on the Stability of Developing Laminar Pipe Flow Subjected to Axisymmetric and Non-Axisymmetric Disturbances, *Journal of Fluid Mechanics*, Vol. 68, Pt. 2 (1975), pp. 345-351.
(9) Schlichting, H. and Gersten, K., *Boundary-Layer Theory, 8th Revised and Enlarged ed*., (2000), p. 419, Springer.
(10) Trefethen, L. N., Trefethen, A. E., Reddy, S. C., and Driscoll, T. A., Hydrodynamic Stability Without Eigenvalues, *Science*, Vol. 261, No. 5121 (1993), pp. 578-584.
(11) Baggett, J. S., Driscoll, T. A., and Trefethen, L. N., A Mostly Linear Model of Transition to Turbulence, *The Physics of Fluids*, Vol. 7, No. 4 (1995), pp. 833-838.
(12) Baggett, J. S., and Trefethen, L. N., Low-Dimensional Models of Subcritical Transition to Turbulence, *The Physics of Fluids*, Vol. 9, No. 4 (1997), pp. 1043-1053.
(13) Shan, H., Zhang, Z., and Nieuwstadt, F. T. M., Direct Numerical Simulation of Transition in Pipe Flow under the Influence of Wall Disturbances, *International Journal of Heat and Fluid Flow*, Vol. 19, Issue 4 (1998), pp. 320-325.
(14) Eckhardt, B., and Mersmann, A., Transition to Turbulence in a Shear Flow, *Physical Review* E, Vol. 60, No. 1 (1999), pp. 509-517.
(15) Meseguer, A., Streak Breakdown Instability in Pipe Poiseuille Flow, *The Physics of Fluids*, Vol. 15, No. 5 (2003), pp. 1203-1213.
(16) Mellibovsky, F., and Meseguer, A., The Role of Streamwise Perturbations in Pipe Flow Transition, *The Physics of Fluids*, Vol. 18, Issue 7, 074104 (2006).
(17) Mellibovsky, F., and Meseguer, A., Pipe Flow Transition Threshold Following Localized Impulsive Perturbations, *The Physics of Fluids*, Vol. 19, Issue 4, 044102 (2007).
(18) Waleffe, F., Transition in Shear Flows. Nonlinear Normality Versus Non-normal Linearity, *The Physics of Fluids*, Vol. 7, Issue 12, (1995), pp. 3060-3066.
(19) Wygnanski, I. J. and Champagne, F. H., On Transition in a Pipe. Part 1. The Origin of Puffs and Slugs and the Flow in a Turbulent Slug, *Journal of Fluid Mechanics*, Vol. 59, Pt. 2 (1973), pp. 281-335.
(20) Wygnanski, I., Sokolov, M., and Friedman, D, On Transition in a Pipe. Part 2. The Equilibrium Puff, *Journal of Fluid Mechanics*, Vol. 69, Pt. 2 (1975), pp. 283-304.
(21) Rubin, Y., Wygnanski, I., and Haritonidis, J. H., Further Observations on Transition in a Pipe, *Laminar-Turbulent Transition*, *IUTAM Symposium Stuttgart 1979* (1980), pp. 17-26, Springer-Verlag.
(22) Bandyopadhyay, P. R., Aspects of the Equilibrium Puff in Transitional Pipe Flow, *Journal of Fluid Mechanics*, Vol. 163 (1986), pp. 439-458.
(23) Darbyshire, A. G., and Mullin, T., Transition to Turbulence in Constant-Mass-Flux Pipe Flow, *Journal of Fluid Mechanics*, Vol. 289 (1995), pp. 83-114.
(24) Matsuuchi, K., and Adachi, T., Generation of Puffs in a Pipe, *Journal of Japan Society of Fluid Mechanics*, Vol. 12, No. 2 (1993), pp. 147-156 (in Japanese).
(25) Kobayashi, T., Hamada, I., and Matsuuchi, K., Necessary Condition of External Disturbances for the Generation of Puffs in a Pipe, *Journal of Japan Society of Fluid Mechanics*, Vol. 18, No. 1 (1999), pp. 47-50 (in Japanese).
(26) Azuma, T., and Araga, K., Generation and Growth of Puff and Slug in Initial Stage of a Transitional Pipe Flow, *Transactions of the Japan Society of Mechanical Engineers*, *Series B*, Vol. 67, No. 654 (2001), pp. 421-429 (in Japanese)

(27) Araga, K., and Azuma, T., Turbulent Puff Produced by a Ring-Shaped Roughness Element in a Pipe Flow, *Transactions of the Japan Society of Mechanical Engineers*, *Series B*, Vol. 68, No. 666 (2002), pp. 300-308 (in Japanese).
(28) Draad, A. A., Kuiken, G. D. C., and Nieuwstadt, F. T. M., Laminar-Turbulent Transition in Pipe Flow for Newtonian and Non-Newtonian Fluids, *Journal of Fluid Mechanics*, Vol. 377 (1998), pp. 267-312.
(29) Hof, B., Juel, A., and Mullin, T., Scaling of the Turbulence Transition Threshold in a Pipe, *Physical Review Letters*, Vol. 91, No. 24, 244502 (2003).
(30) Hof, B., Transition to Turbulence in Pipe Flow, *IUTAM Symposium on Laminar-Turbulent Transition and Finite Amplitude Solutions* (2005), pp. 221-231, Springer.
(31) Mullin, T., and Peixinho, J., Recent Observations of the Transition to Turbulence in a Pipe, *Sixth IUTAM Symposium on Laminar-Turbulent Transition* (2006), pp. 45-55, Springer.
(32) Peixinho, J., and Mullin, T., Finite-Amplitude Thresholds for Transition in Pipe Flow, *Journal of Fluid Mechanics*, Vol. 582 (2007), pp. 169-178.
(33) Kanda, H., Numerical Study of the Entrance Flow and Its Transition in a Circular Pipe, *The Institute of Space and Astronautical Science Report*, No. 626, (1998).
(34) Zanoun, E.-S., Kito, M., and Egbers, C., A Study of Flow Transition and Development in Circular and Rectangular Ducts, *Transactions of the ASME, Journal of Fluids Engineering*, Vol. 131, Issue 6, 061204 (2009).
(35) Lessen, M., Fox, J. A., Bhat., W. V., and Liu, T. -Y., Stability of Hagen-Poiseuille Flow, *The Physics of Fluids*, Vol. 7, No. 8 (1964), pp. 1384-1385.
(36) Durst, F., and Ünsal, B., Forced Laminar-to-Turbulent Transition of Pipe Flows, *Journal of Fluid Mechanics*, Vol. 560 (2006), pp. 449-464.
(37) Nishi, M, Ünsal, B., Durst, F., and Biswas, G., Laminar-to-Turbulent Transition of Pipe Flows Through Puffs and Slugs, *Journal of Fluid Mechanics*, Vol. 614 (2008), pp. 425-446.
(38) Ichimiya, M., Abe, T., Fukutomi, J., and Kondo, M., Laminar-Turbulent Transition of a Boundary Layer Induced by a Single Roughness Element in an Inlet Region of a Circular Pipe Flow (Developing Process of a Stationary Turbulent Region), *Transactions of the Japan Society of Mechanical Engineers*, *Series B*, Vol. 73, No. 725 (2007), pp. 154-161 (in Japanese).
(39) Ito, H., Watanabe, Y., and Shoji, Y., A Long-Radius Inlet Nozzle for Flow Measurement, *Journal of Physics*, *E*: *Scientific Instruments*, Vol. 18, No. 1 (1985), pp. 88-91.
(40) Hedley, T. B., and Keffer, J. F., Turbulent/Non-Turbulent Decisions in an Intermittent Flow, *Journal of Fluid Mechanics*, Vol. 64. Pt. 4 (1974), pp. 625-644.
(41) Murlis, J., Tsai, H. M., and Bradshaw, P., The Structure of Turbulent Boundary Layers at Low Reynolds Numbers, *Journal of Fluid Mechanics*, Vol. 122 (1982), pp. 13-56.
(42) Kuan, C. L., and Wang, T., Investigation of the Intermittent Behavior of Transitional Boundary Layer Using a Conditional Averaging Technique, *Experimental Thermal and Fluid Sciences*, Vol. 3, Issue 2 (1990), pp. 157-173.
(43) Tatsumi, T., Stability of the Laminar Inlet-flow Prior to the Formation of Poiseuille Regime, I, *Journal of the Physical Society of Japan*, Vol. 7, No. 5 (1952), pp. 489-495.
(44) Kanda, H., and Shimomukai, K., Numerical Study of Pressure Distribution in Entrance Pipe Flow, *Journal of Complexity*, Vol. 25, Issue 3 (2009), pp. 253-267.
(45) The Japan Society of Mechanical Engineers, *JSME Data Book*, *Hydraulic Losses in Pipes and Ducts*, (1979), p. 23, Maruzen (in Japanese).
(46) Schubauer, G. B., and Klebanoff, P. S., Contributions on the Mechanics of Boundary-Layer Transition, *NACA Report*, No. 1289 (1956).
(47) Duguet, Y., Willis, A. P., and Kerswell, R. R., Slug Genesis in Cylindrical Pipe Flow, *Journal of Fluid Mechanics*, Vol. 663 (2010), pp. 180-208.